Vacuum ultraviolet photochemistry of CH$_4$ and isotopomers. II. Product channel fields and absorption spectra

Jen-Han Wang and Kopin Liu
Institute of Atomic and Molecular Science (IAMS), Academia Sinica, Taipei, Taiwan 10764

Zhiyuan Min, Hongmei Su, and Richard Bersohn
Department of Chemistry, Columbia University, New York, New York 10027

Jack Preses and John Z. Larese
Chemistry Department 555A, Brookhaven National Laboratory, Upton, New York 11973

In part I of this work the relative velocities and anisotropies of the atomic H and D fragments from methane photolysis at 10.2 eV were measured. In this paper the relative abundance of the methyl and methylene fragments are reported. A complete set of quantum yields for the different photodissociation channels of each isotopomer is obtained by combining the two sets of data. Previously it was found that H atoms are almost four times more likely than D atoms to be ejected; now it is found that hydrogen molecule photofragments are much richer in H atoms than in D. Overall, the heavier D atoms are more likely than the H atoms to remain attached to the carbon atom. An implication for astrophysics is discussed. The VUV absorption spectra of CH$_4$ and CH$_3$D are almost identical both at room temperature and 75 K. There is, as expected, no variation in the absorption spectrum with temperature. Evidence is given that all or almost all of the methylene is produced in the $a\ ^1A_1$ and not in the ground $^3B_1$ state. © *2000 American Institute of Physics.* [S0021-9606(00)00934-X]

I. INTRODUCTION

Methane is the most abundant hydrocarbon on earth and is present in small amounts in the atmospheres of all the planets. For example, in the atmosphere of Jupiter its mole fraction is about 2×10^{-3}.[1] Other hydrocarbons are even less abundant. The most remarkable exception is the atmosphere of Titan, the largest moon of Saturn which has 2%–3% methane and heavier hydrocarbons as well. The observations of Titan made by the Voyager space craft are tantalizing but incomplete.[2] A new space craft, Cassini, is on its way and is expected to reach Saturn in 2004. In order to construct a photochemical model for this atmosphere, it is essential to know the yields of the different photodissociation channels at 121.6 nm (10.2 eV). The yields are also of intrinsic interest for the theory of photodissociation of small molecules. The choice of photon wavelength is determined by two closely linked considerations. Nearly 92% of the solar VUV radiation absorbed by methane is due to the $2p$-$1s$ emission of H atoms, the Lyman α line.[3] This same transition is used as a laboratory detector for the hydrogen atoms produced by absorption.

The electronic absorption of methane begins only around 140 nm ($\sim$8.8 eV).[4] The VUV spectrum consists of two not well-resolved humps which were at one time assigned to two different electronic transitions. Recent *ab initio* calculations by Mebel *et al.* have finally revealed the nature of the spectrum.[5] The absorption from 9 to 12 eV is due to a transition to a single, triply degenerate excited state, $^1T_2$. The excited state correlates to CH$_2$($b\ ^1B_1$)+H$_2$ which is a very minor channel with yield $\leq$2%. However, on the excited potential surface are minima with C_{3V} or C_{2V} symmetry. These minima are not stable because surface crossing is

rapid. Photodissociation of methane is therefore mainly an indirect process in that dissociation does not take place from S_1 but from the triplet T_1 state or from the S_0 ground state. The triplet state can correlate only to CH$_3$+H, whereas the ground state can correlate to CH$_3$+H as well as to CH$_2$($a\ ^1A_1$)+H$_2$.

Because there is a large excess energy in the nine normal modes of the molecule and an extensive reorganization of all the normal modes on the excited surface occurs, the spectrum consists of thousands of weak vibronic transitions. Mebel *et al.* showed that the two broad humps and the small bumps are accidental bunches of transitions. They have no simple physical meaning.

The previous paper (part I) reported the hydrogen atom yields, velocity distributions, and anisotropy parameters in the photodissociation of CH$_4$, CH$_3$D, CH$_2$D$_2$, and CHD$_3$.[6] The present paper describes the measurement of the relative yields of methylene and methyl radicals derived from the methane isotopomers. With the help of some assumptions, a complete table of quantum yields is obtained. In addition, the absorption spectrum of CH$_4$ and CH$_3$D have been measured both at room temperature and 75 K. Finally, the atomic H/D ratio at 118.2 nm is reported.

II. EXPERIMENT

A. Total quantum yield for H atoms from CH$_4$ (Columbia)

The total quantum yield of H atoms is determined by measuring the ratio of the areas under the laser-induced fluorescence excitation curves of CH$_4$ and another molecule with known quantum yield. H$_2$O is chosen because it has a unit quantum yield. The experiment is a one-color experiment in

that the Lyα is used both to dissociate and to probe the H atom photoproduct. The Lyα was generated by mixing two photons at 212.6 nm resonant with a two photon transition and a third photon around 845 nm in a Kr cell containing Ar. The optimum amount of Ar depends on the laser intensity so it has to be optimized with each run. The signals from methane and water vapor were measured six times alternately with water at 80 mTorr and methane at 50 mTorr. The signals were normalized to equal pressures and corrected for absorption of the exciting light and the emitted light within the 8 cm cubic cell.

B. Photoionization yield measurements (IAMS)

The experiment was carried out in a crossed-beam apparatus as detailed in part I. The VUV laser at 121.6 nm, which served as both the photolysis and the fragment ionization photon sources, was generated by a frequency tripling process in a Kr gas cell. To avoid other multiphoton complications, the VUV laser beam was unfocused. It had the dimensions ~ 3 mm$\times 5$ mm through the interaction region and the more intense UV beam (364.8 nm, <4 mJ/pulse) diverged. The ion TOF mass spectrometer was operated in the usual mass mode. The slit aperture, which was used in part I for velocity measurement, was removed to ensure the detection of all ions. Research grade $CH_4(99.99\%)$ and isotopomers (98% from Cambridge Isotope Lab.) were used as received. The supersonically cooled beam was composed of 20% CH_4 or its isotopomer in He with a total backing pressure of 2 atm. To ensure that the beam is free of clusters, the laser was timed to fire at the leading part of the pulsed beam. The VUV photoionization mass spectra were acquired with the molecular beam on and off, as described in Ref. 7. Over the mass range of this work, the spectra are essentially background free. The integration of each peak, to account for the small difference in width, gives the relative ion yields. The normalization of the photoionization yield spectra for different isotopomers was carried out by several back-to-back measurements.

C. Absorption spectra (Brookhaven)

The absorption spectra of $CH_4(99\%)$ and $CH_3D(98\%)$ (from Cambridge Isotope Lab.) were measured using the U11 beam line of the National Synchrotron Light Source at Brookhaven National Laboratory. A 10 cm long cell was used with LiF windows and a 0.1 nm resolution. The corresponding optimal room temperature pressures for methane were ~ 0.2 Torr. A program available at the beam line was used to derive VUV absorption spectra[8] from recordings of VUV transmission through the cell with and without methane. The program made appropriate normalizations for variations in source intensity and absorption spectra were derived from the measurements. Low temperature was maintained by cooling the cell to 75 K with a closed cycle He cryostat. Because of temperature variations between the cold cell and the warm capacitance manometer used to measure pressure, molar extinction coefficients could not be determined quantitatively at low temperature.

D. Atomic H/D ratios from methane isotopomers at 118.4 and 121.6 nm (Columbia)

All experiments were carried out inside an 8 cm cubic stainless steel cell. Lyα light was generated by four-wave mixing of a fixed 212.6 nm wavelength with a tunable wavelength near 845 nm. The pressure of methane was 60 mTorr. The H/D ratios from the isotopomers CH_nD_{4-n} were measured at two VUV wavelengths under two very different conditions. When Lyα was both the dissociating and probing light, it was naturally made as intense as possible. The counterpropagating 118.4 nm light was made by focusing the third harmonic, 355 nm of a YAG laser in a mixture of 5 Torr of xenon and 70 Torr of argon. The observed signal was the sum of a signal proportional to the product of the 118.4 nm intensity times the Lyα intensity plus a signal quadratic in the Lyα intensity. Under these conditions the Lyα intensity was reduced so that the quadratic effect was 20%–30% of the main signal. The probe laser was scanned through the absorption of both H and D and then the 118.4 nm laser was blocked and the spectrum run again. The second spectrum was subtracted from the first and the cell was filled with a fresh gas sample. The uncertainty quoted in the final result is the rms deviation of the six repetitions of this process. An additional change in conditions was necessary because of the high velocity of the hydrogen atoms produced and the often large variation in the long 500 ns time delay between the YAG based dissociating laser and the excimer pumped dye based Lyα. To prevent selective loss of the faster H atoms, 800 Torr of helium was added. The helium does not quench the H atom fluorescence and the high pressure keeps the atoms from migrating out of the probe beam.

III. RESULTS AND DISCUSSION

A. Electronic state of methylene photofragment

There are two distinct observations. One is that when irradiating with 10.2 eV photons, ion signals appear due to CH_2^+ and its isotopomers. The second is that when a gas containing methane and a hundredfold excess of N_2 is irradiated at 118.2 nm (10.49 eV), a large IR absorption appears due to C_2H_4. If the N_2 is replaced by H_2, there is no detectible C_2H_4.

Methylene could, in principle, be formed in either the ground $X\,^3B_1$ state or the first excited $a\,^1A_1$ state, 3156 ± 5 cm^{-1} higher. At the outset, we wish to present evidence that some of the CH_2 is produced in the $a\,^1A_1$ state and some additional evidence that almost all of it is. The ionization potential of $CH_2(X)$ is 10.3962 ± 0.0036 eV and that of $CH_2(a)$ is 10.005 eV.[9] The Lyman alpha photon whose energy is 10.199 eV can ionize $CH_2(a)$ but not $CH_2(X)$. The ion signals seen of CH_2^+ and of its isotopomers are therefore due to methylene in the a state.

The photochemical result implies that all or almost all the CH_2 is formed in the a state. $CH_2(a)$ is readily quenched by N_2 to $CH_2(X)$. The process

$$CH_2(a\,^1A_1)+N_2\rightarrow[H_2CNN]\rightarrow CH_2(X\,^3B_1)+N_2$$

is analogous to the very efficient isoelectronic reaction:

TABLE I. Photoion signal strengths (arbitrary un) of various mass peaks at 10.2 eV photon energy.

M/e	CH_4	CH_3D	CH_2D_2	CHD_3
14	1.52	0.666	0.173	
15	0.62	0.952	0.957	0.685
16		0.608	0.590	0.948
17			0.354	0.156
18				0.192

$$O(^1D) + N_2 \rightarrow [NNO] \rightarrow O(^3P) + N_2.$$

When H_2 replaces N_2, it reacts easily with the nascent energized singlet methylenes through a methane transition state just as $O(^1D)$ reacts rapidly with H_2 through an intermediate H_2O transition state.

B. Photofragment yields

The observed ion signals for each isotopomer are listed in Table I. These are not the relative yields because we do not know the ratio, designated x, of the ionization cross section for CH_2 to that for CH_3, $\sigma(10.2)_{CH_2}/\sigma(10.2)_{CH_3}$. We deduce the value of x from the previous detailed results on hydrogen atom velocity distributions and yields from the photodissociation of methane and its isotopomers at 10.2 eV.[6] It turns out that the two ionization cross sections are almost equal, so that Fig. 1 gives at a glance a picture of the relative methyl and methylene yields.

There is extensive literature dealing with the classical photochemistry of methane.[10–12] The gas is irradiated with a lamp for a certain period of time, the products are analyzed and the elementary processes are deduced. If all the products were stable molecules, the backward step from the composition of the irradiated gas to the elementary processes would be simple. Unfortunately, besides stable molecules, the products include reactive intermediates such as atoms, radicals, and carbenes which react with each other as well as the parent molecules. Moreover, their reaction rates often depend
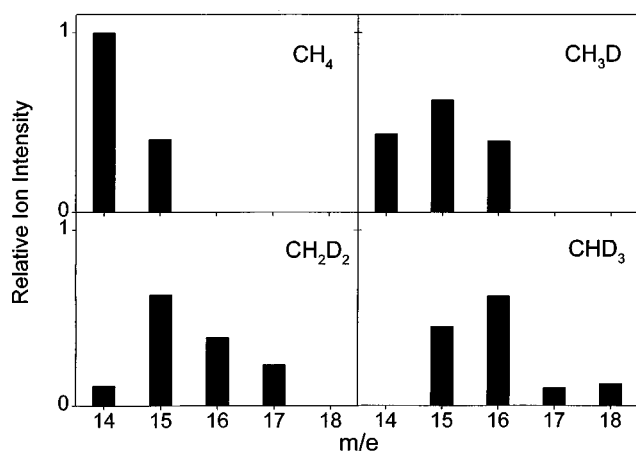

FIG. 1. A bar graph of the data of Table I showing relative ion signals of the photofragments of methane and its isotopomers irradiated at 10.2 eV. All ion signals are on the same arbitrary scale.
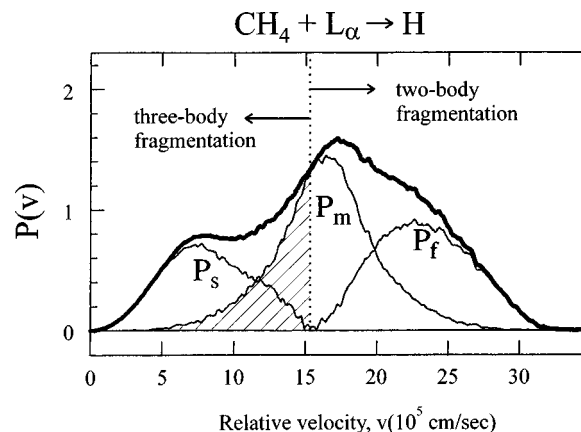

FIG. 2. The relative velocity distribution for H atoms photodissociated at 10.2 eV from CH_4. The two peaked distribution is decomposed into a fast, medium, and slow distribution (see text and part I).

on their translational and internal energies. Direct measurement of the nascent products when laser-based methods are available is highly desirable.

For methane, four important dissociation channels have been found:

$$CH_4 + h\nu \rightarrow CH_3 + H \tag{1a}$$

$$\rightarrow CH_2(a\,^1A_1) + H_2 \tag{1b}$$

$$\rightarrow CH_2(a\,^1A_1) + H + H \tag{1c}$$

$$\rightarrow CH + H_2 + H. \tag{1d}$$

In part I it was found that the translational energy distributions of H and D atoms from all the isotopomers are bimodal having a low energy and a high energy peak (see Fig. 21). At first, hydrogen atoms are divided into two classes: those with so much translational energy that a three-body dissociation is energetically impossible and those moving slowly enough that three-body dissociations are possible. The threshold for channels c and d are 9.23 and 9.05 eV, respectively. We assume therefore that all atoms with energies <1.15 eV result from a three-body dissociation. As shown in Fig. 2, this assumption means that the area under the first peak and a lower energy side of the area under the second peak are assigned to three-body dissociations.

The product hydrogen atoms can be subdivided according to whether they could or could not be a product of a three-body dissociation. Another subdivision is based on the speed dependent anisotropy parameter, β. As explained in part I, the speed distributions can be fitted by a sum of three distributions, labeled fast, medium, and slow. The fast distribution has a $\beta = -0.45$, the medium distribution has a β which is close to 2 at high energy but diminishes to zero at low energy. The third slow component has a β close to zero. Table III in part I lists the fraction of the H and D atoms assigned to the three categories. Figure 2 shows the decomposition for methane.

The a channel has, in effect, been divided into two channels, "fast" and the higher energy part of the "medium." The fastest hydrogen atoms which have a constant negative β are believed to dissociate at the earliest time. The medium

TABLE II. Relative H and D ion signals, partitioned between two-and three-body fragmentation. These numbers were obtained from the areas of Figs. 7 and 9 of Ref. 6 above and below the threshold for three-body dissociation. Signals are normalized to unity for CH_4.

Channel	CH_4	CH_3D	CH_2D_2	CHD_3
Two fragment H atom	0.620	0.608	0.355	0.192
Three fragment H atom	0.380	0.363	0.165	0.061
Two fragment D atom		0.032	0.071	0.156
Three fragment D atom			0.058	0.094

TABLE III. Photodissociation channels of methane isotopomers. The sum of the yields for any molecule is, by definition, one but the closeness of the sum to one is used in Tables IV and VI as a check on overall consistency.

CH_3D	Yield	CHD_3	Yield	CH_2D_2	Yield
CH_2D+H	$a1$	CHD_2+D	$a1'$	CHD_2+H	$a1''$
CH_3+D	$a2$	CD_3+H	$a2'$	CH_2D+D	$a2''$
$CHD+H_2$	$b1$	$CHD+D_2$	$b1'$	CD_2+H_2	$b1''$
CH_2+HD	$b2$	CD_2+HD	$b2'$	$CHD+HD$	$b2''$
				CH_2+D_2	$b3''$
$CHD+H+H$	$c1$	$CHD+D+D$	$c1'$	CD_2+H+H	$c1''$
CH_2+H+D	$c2$	CD_2+H+D	$c2'$	$CHD+H+D$	$c2''$
				CH_2+D+D	$c3''$
$CH+HD+H$	$d1$	$CD+HD+D$	$d1'$	$CD+HD+H$	$d1''$
$CD+H_2+H$	$d2$	$CH+D_2+D$	$d2'$	$CH+D_2+H$	$d2''$
$CH+H_2+D$	$d3$	$CD+D_2+H$	$d3'$	$CH+HD+D$	$d3''$
				$CD+H_2+D$	$d4''$

hydrogen atoms have a broader speed distribution, and a β which decreases with decreasing energy. Hydrogen atoms with lower speeds are formed simultaneously with methyls with more internal energy. The dissociation process probably takes progressively longer. When the atom has a kinetic energy $<1.15\,eV(15\times10^5\,cm/s)$, the methyl radical partner has enough energy to dissociate into $CH+H_2$. We assume that this channel switches on immediately above threshold because the reaction $CH+H_2\rightarrow CH_3$ is facile, i.e., there is an angle of approach for which there is no barrier to reaction and therefore there is no barrier for the reverse reaction.[12]

Calculation of absolute quantum yields proceeds as follows. Let the quantum yields of these four channels be denoted by a, b, c, and d, respectively. By definition,

$$a+b+c+d=1. \quad (2)$$

The total quantum yield for H atom production has been found by Brownsword et al. to be 0.47 ± 0.11.[13] We have independently measured the same yield as described in the experiment section. The ratio of the signal from H_2O to that from CH_4 was 1.77 ± 0.05 and the ratio of the absorption coefficient of H_2O to that of CH_4 is $(1.6\pm0.1)/(2.0\pm0.1)=0.80\pm0.08$. The total quantum yield assuming unit quantum yield for water is 0.45 ± 0.10, insignificantly different from the prior result. We can then write:

$$a+2c+d=y, \quad where \quad y \quad is \quad 0.47\pm0.11. \quad (3)$$

From Table I we can write the ratio of the CH_2^+ signal to that of the CH_3^+:

$$x(b+c)/a=1.52/0.62=2.452. \quad (4)$$

In other words, the ratio of the ion signals is equal to the ratio of the quantum yield for producing CH_2 to that for CH_3 times the ratio of the photoionization cross sections, x.

Table II contains a set of ion signals from H and D atoms partitioned between those from two or three-body fragmentation. The normalization is such that the total H atom signal from CH_4 is taken as unity. However, the total quantum yield for H atoms from CH_4 is y. Therefore, the quantum yield for H atoms produced by the two-body channel is

$$a=0.62y. \quad (5)$$

Equations (2)–(4) can be solved for the individual quantum yields b, c, and d in terms of x and y;

$$b=0.760y/x-y/2+1/2, \quad (6)$$

$$c=0.760y/x+y/2-1/2, \quad (7)$$

$$d=1-0.62Y-1.520y/x. \quad (8)$$

To evaluate the unknown x, the ratio of the photoionization cross section of CH_2 to that of CH_3, one additional assumption is necessary. This is that the d channel H atoms are the low energy tail of the "medium" component of the H atom translational energy distribution. If so, the "slow" component H atoms must be assigned to the c channel. Referring to Table III of part I, the slow component is a fraction 0.232 of the total H atom yield. Therefore, $2c=0.232y$ is an additional equation which allows x to be obtained. If $c=0.116y$, then

$$x=1.520y/(1-0.768y). \quad (9)$$

If $y=0.47\pm0.11$, then $x=1.118\pm0.420$

Substituting these values of x and y in Eqs. (5)–(8), one obtains the absolute yields:

$$a=0.291\pm0.068,$$
$$b=0.585\mp0.098,$$
$$c=0.066\pm0.012, \quad (10)$$
$$d=0.068\pm0.013.$$

The uncertainties included in the above quantum yields are those due to the ±0.11 uncertainty in y, the total quantum yields for producing H atoms. The measurement of y is quite independent of the measurements reported here and in part I. Moreover, x could be independently measured. Thus it is hoped that future investigators could use Eqs. (5)–(8) with improved values of x and y.

The various channels for the dissociation of the isotopomers, CH_nD_{4-n} are listed in Table III. The absolute yields listed in Table IV were calculated using all of the following data

(1) The "slow" component fractions of the total H and D atom velocity distributions using the data in Table III of part I.
(2) The ratios of two-fragment to three-fragment yields (Table II) deduced from the areas of Figs. 7 and 9 of Part I above and below $v=15\times10^5$ cm/s.
(3) The H/D ratios from Table IV of part I.

(4) The ion signal ratios of the various fragment masses derived from each molecule of Table I using $x = 1.118$; and

(5) The ratio of a unique methyl ion signal from an isotopomer to that of methane.

Table IV lists the yields of the different photodissociation channels. Table V lists the yields of specific isotopomers of the methylene and methyl fragments. The overall picture is obtained from Table VI which lists just the four yields from each chemically distinct channel. The sum of the four yields for methane has been normalized to one. The sum of the yields of the other isotopomers has *not* been normalized. The fact that the sum of their yields is close to one supports the assumptions used in partitioning the hydrogen atom velocity distributions. No correction has been applied for the different coefficients for absorption of the 10.2 eV light.

Hydrogen molecules were not directly probed in these experiments but the relative yields of H_2, HD, and D_2 can be determined approximately. The following equations give the yields of the three hydrogen molecule isotopomers using Tables II and IV.

For CH_3D,

$$\phi_{H_2} = b1 + d2 + d3 = 0.334 + <0.063,$$

$$\phi_{HD} = b2 + d1 = 0.271 + <0.054.$$

For CHD_3,

$$\phi_{HD} = b2'd1' = 0.379 + <0.025,$$

$$\phi_{D_2} = b1' + d2' + d3' = 0.287 + <0.010.$$

For CH_2D_2,

$$\phi_{H_2} = (b1'' + c1'') - c1'' + d4''$$

$$= 0.218 - <0.020 + <0.027,$$

$$\phi_{HD} = (b2'' + c2'') - c2'' + d1'' + d3''$$

$$= 0.402 - <0.014 + <0.064,$$

$$\phi_{D_2} = (b3'' + c3'') - c3'' + d2''$$

$$= 0.073 - <0.014 + <0.037.$$

The inequalities appear in the above equations because the small d and c'' coefficients have not been individually determined. From CH_3D on statistical grounds H_2 and HD should be formed in equal numbers. The experimental

TABLE V. Photoionization yields of the observed molecular fragments at 10.2 eV photon energy.

Fragment	CH_4	CH_3D	CH_2D_2	CHD_3
CH_2	0.619	0.280	0.073	
CH_3	0.291	0.015		
CHD		0.387	0.402	0.288
CH_2D		0.286	0.033	
CD_2			0.218	0.399
CHD_2			0.167	0.073
CD_3				0.090

H_2/HD ratio is ~1.23. Similarly from CHD_3, HD and D_2 should be formed in equal numbers but the HD/D_2 ratio is ~1.32. Finally, CH_2D_2 should form H_2, HD, and D_2 in a 1:4:1 ratio but the observed ratio is 1:1.85:0.33.

In part I an important photochemical discovery was that the atomic H/D ratio from a molecule CH_nD_{4-n} was three to four times the statistically expected ratio $[n/(4-n)]$. We now find that the abundance of H atoms in hydrogen molecules is also highly nonstatistical. A broad qualitative explanation is that the intramolecular forces acting on H and D atoms are the same but the H atoms have, classically, twice the acceleration. This means that an H atom under the action of a force will pass the point of no return sooner than a D atom subjected to the same force. However, there are two kinds of points of no return. If the force is predominantly radial, the atom which passes a certain C–H separation becomes a free atom. If the force is predominantly angular, the point of no return is an atom–atom distance less than which a hydrogen molecule has been formed. Obviously forces are not purely radial or angular. The mixed directions produce hydrogen atoms with reduced β. It would also follow that there is not a unique C–H or H–H distance beyond which there is product formation. This is a zero order explanation which needs further theoretical elaboration. It must be emphasized that once the H and D atoms really leave the molecule, they are detected with equal probability.

The overall results in Table VI can be compared with previous photochemical studies done on CH_4 and CD_4.[8–10] Substantial isotope effects on the yields of different channels were found. Fewer atoms are released by CD_4 than by CH_4. Less CD is formed from CD_4 than CH from CH_4. These conclusions are now seen to be part of a continuous trend with the number of deuterium atoms in the molecule. The hydrogen atom yield steadily decreases with increasing deu-

TABLE IV. Quantum yields of isotopically distinct product channels.

CH_4	CH_3D	CH_2D_2	CHD_3
0.291(a)	0.286($a1$)	0.166($a1''$)	0.073($a1'$)
0.585(b)	0.015($a2$)	0.034($a2''$)	0.090($a2'$)
0.055(c)	0.334($b1$)	0.218($b1''+c1''$)	0.287($b1'$)
0.070(d)	0.271($b2$)	0.402($b2''+c2''$)	0.379($b2'$)
	0.054($c1$)	0.073($b3''+c3''$)	0.000($c1'$)
	0.009($c2$)	0.037($d1''+d2''$)	0.019($c2'$)
	0.054($d1+d2$)	0.027($d3''+d4''$)	0.25($d1'+d2'$)
	0.008($d3$)	0.040($2c1''+c2''$)	0.010($d3'$)
		0.014($2c3''+c2''$)	

TABLE VI. Fractional yields of four chemically distinct product channels. X denotes H or D and X_2 denotes H_2, HD, or D_2.

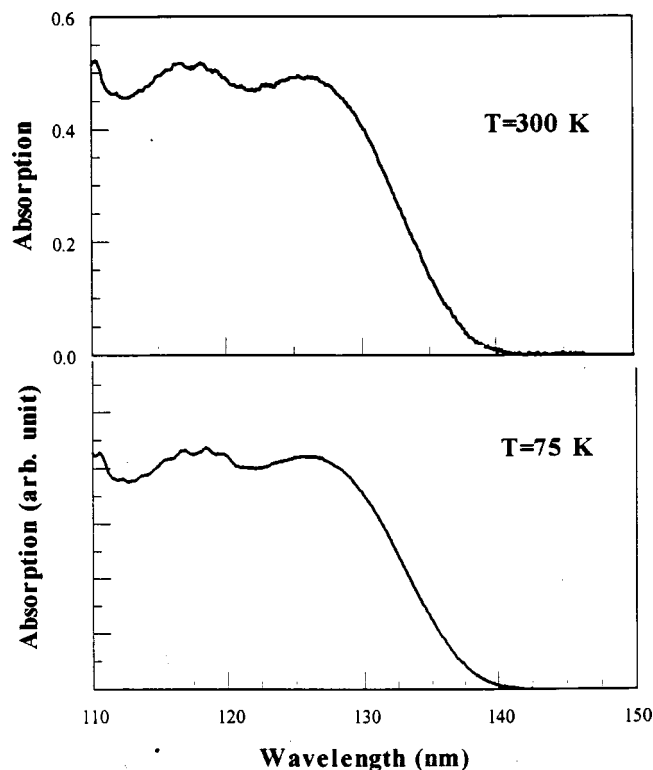| Channel	CH_4	CH_3D	CH_2D_2	CHD_3
(a) CX_3+X	0.291	0.301	0.200	0.163
(b) CX_2+X_2	0.584	0.605	0.665	0.667
(c) CX_2+X+X	0.055	0.063	0.027	0.019
(d) $CX+X_2+X$	0.070	0.063	0.065	0.035
Total yield	1.000	1.032	0.957	0.884
X yield	0.470	0.490	0.319	0.236
X_2 yield	0.654	0.668	0.730	0.702
X/X_2	0.719	0.734	0.437	0.336

FIG. 3. Absorption spectra of CH_4 at 300 K and at 75 K. The cell was 10 cm in length and the pressure was 0.192 Torr. Absorption in Figs. 3 and 4 is $\ln(I/I_0)$.

teration and, to compensate, the hydrogen molecule yield steadily increases. In general, the D atom is more likely than the H atom to remain bonded to the carbon atom. The process of dissociation is very likely slower when the masses in the system are doubled. The lighter atoms are preferentially ejected either as atoms or as diatomic molecules.

A corollary to the statement that D atoms preferentially remain attached to the carbon atom is that subsequent reaction products such as ethane and ethylene will be richer in D atoms than the original methane. This means that the hydrocarbon molecules found in the atmosphere of Titan, a moon of Saturn will be enriched in D compared to methane if, in fact, they are derived from methane through an initial photodissociation.[14]

C. Absorption spectra of CH_4 and CH_3D at room *T* and at 75 K

The calculation of Mebel *et al.* has shown that the shape of the VUV spectrum of methane has no obvious physical interpretation. It is nevertheless interesting to see if there is any modification of the spectrum caused by lowering the temperature or by isotopic substitution. The absorption of cold methane is important for obvious astrophysical reasons as well as because nozzle-expanded supercold molecular beams are used in research. The question has been raised as to whether the absorption of methane is the same at low temperatures as at room temperature.[15] Because of pressure instabilities at low temperatures in our apparatus, we were not able to measure an absolute absorption of cold methane but, as shown in Fig. 3, the spectrum has exactly the same
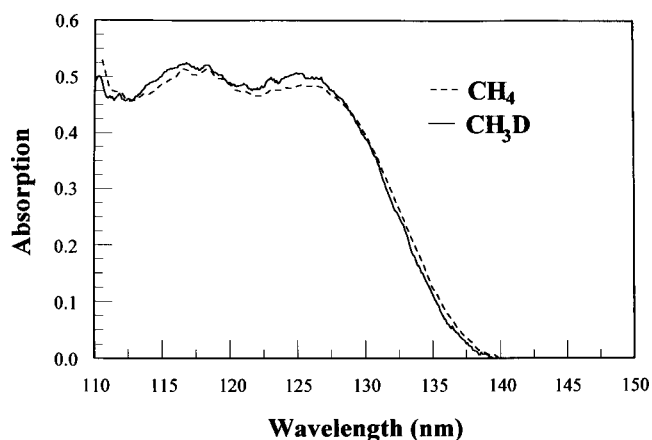

FIG. 4. Room temperature absorption spectra of CH_4 and CH_3D at 0.192 Torr.

shape at 75 K as at room temperature. This is not a surprise because at room temperature only 0.7% of methane molecules are in an excited vibrational state. Only these molecules would be expected to have different absorption coefficients at the two temperatures. In any case, even the small protuberances on top of the larger two peaks are reproduced at low temperature and are therefore not due to rotations.

Some time ago, somewhat coarse-grained spectra of CH_4 and CD_4 were reported which showed that at 10.2 eV CD_4 absorbed about 20% more strongly than CH_4.[16] We have measured the spectra of CH_3D and found, as shown in Fig. 4, that the spectrum is almost identical in shape and strength to that of CH_4. This means that isotope dependent absorption does not play a significant role in the photochemistry of naturally occurring methane.[17] As with CH_4, the room temperature and 75 K absorption spectrums of CH_3D have exactly the same shape.

D. Atomic H/D ratios at 118.4 and 121.6 nm

The results of the LIF measurements of atomic H/D yields from photodissociation at 121.6 and 118.4 nm are shown in Table VII. The ratios obtained at 121.6 nm indicate
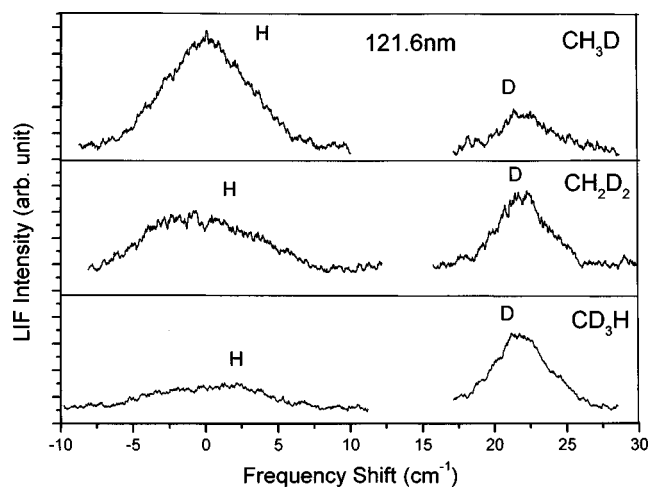

FIG. 5. LIF excitation spectra at 121.6 nm of H and D atoms from photodissociation of methane isotopomers at 121.6 nm.
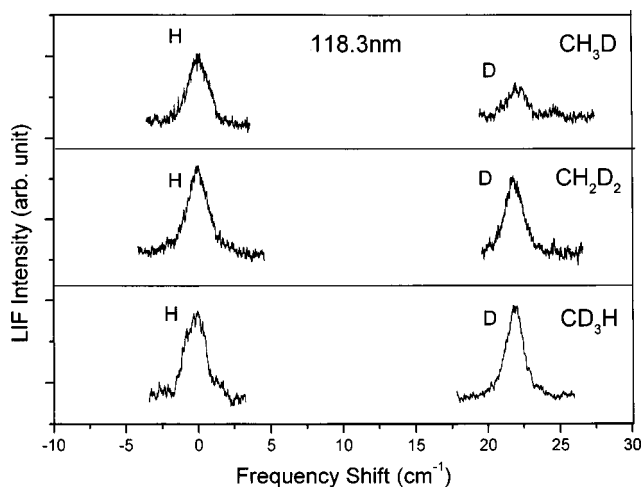
FIG. 6. LIF excitation spectra at 121.6 nm of H and D atoms from photodissociation of methane isotopomers at 118.4 nm in one atm of helium. The weaker spectra from 121.6 nm alone have been subtracted.

TABLE VII. H/D from methane isotopomers at 118.4 and 121.6 nm. The third and fifth columns are obtained by dividing the second and fourth columns by the statistical H/D ratio.

	118.4 nm		121.6 nm	
CH_3D	2.83 ± 0.15	0.94 ± 0.05	4.4 ± 0.4	1.47 ± 0.13
CH_2D_2	1.68 ± 0.08	1.68 ± 0.08	1.58 ± 0.05	1.58 ± 0.05
CHD_3	1.01 ± 0.05	3.03 ± 0.15	0.53 ± 0.03	1.59 ± 0.09

that there is per atom a roughly constant preference for H atom escape by a factor of 1.55 ± 0.10. This is in qualitative but not quantitative accord with the molecular beam RAMP results of Ref. 6, which were used to calculate Table IV. The latter indicated a preference for H atom escape in the range of three to 4.7. We cannot at present identify the reason for the difference in the two sets of data acquired with different methods. If the LyαH/D ratios of Table VII are used to calculate the yields of different channels instead of those in Ref. 1, only the yields, $a2$, $a2'$, and $a2''$ are appreciably affected. The yield $a2$ becomes 0.047. The qualitative result is in line with previous findings on a number of hydrocarbons.[18] When dissociation is from an excited state, dynamics favors the release of the swifter H atom; from an equilibrated ground state statistics favors the release of the more weakly bound H atom because of its higher zero point energy.

Figures 5 and 6 are the LIF spectra of the H and D atoms dissociated from the partially deuterated methanes. The spectra of Fig. 5 were obtained from low pressure methanes. In Fig. 6 one atmosphere of He is added to thermalize the nascent hydrogen atoms. The atoms can no longer escape from the laser beam during the necessary delay time; the spectra are sharpened and thereby the S/N is greatly improved.

The results at 118.4 nm are surprising. In CH_3D there is no preference for H atom release but that preference grows strongly with increasing numbers of deuterium atoms. The absorption spectrum is nearly flat between 10.20 and 10.47 eV (118.4 nm) which does not suggest any drastic change in dynamics. There is one hint in that the weak CH_2 $b \rightarrow a$ emission is increasing rapidly as the energy increases.[4] According to the theory of Mebel *et al.* the upper electronic state of methane correlates at long distances to $CH_2(^1B_1)$ $+ H_2$. As the emission yield increases, the sum of the intersystem and internal conversion rates must decrease. The upper state is becoming slightly less strongly coupled to lower states as the energy increases. The whole question certainly deserves further investigation.

ACKNOWLEDGMENTS

[1] S. K. Atreya, M. H. Wong, T. C. Owen, P. R. Mahaffy, H. B. Niemann, J. dePater, P. Drossart, and Th. Encrenaz, Planet. Space Sci. **47**, 1243 (1999).
[2] D. F. Strobel, M. E. Summers, and X. Zhu, Icarus **100**, 512 (1992).
[3] S. K. Atreya, S. G. Edgington, Th. Encrenaz, and A. H. Feuchtgruber, Proceedings of the Conference ''The Universe as seen by ISO'' (European Space Agency SP-427, March 1999), p. 149.
[4] L. C. Lee and C. C. Chiang, J. Chem. Phys. **78**, 688 (1983).
[5] A. M. Mebel, S.-H. Lin, and C.-H. Chang, J. Chem. Phys. **106**, 2612 (1997).
[6] J.-H. Wang and K. Liu, J. Chem. Phys. **109**, 7105 (1998).
[7] L. H. Lai, Y.-T. Hsu, and K. Liu, Chem. Phys. Lett. **307**, 385 (1999).
[8] J. C. Sutherland, P. C. Keck, K. P. Griffin, and P. Z. Tacacs, Nucl. Instrum. Methods **195**, 375 (1982).
[9] B. Ruscic, M. Litorja, R. L. Asher, J. Phys. Chem. A **103**, 8625 (1999).
[10] A. H. Laufer and J. R. McNesby, J. Chem. Phys. **49**, 2272 (1968).
[11] P. J. Ausloos and S. G. Lias, Annu. Rev. Phys. Chem. **22**, 85 (1971); R. Gorden, Jr. and P. Ausloos, J. Chem. Phys. **46**, 4823 (1967).
[12] R. G. Macdonald and K. Liu, J. Chem. Phys. **93**, 2443 (1990).
[13] R. A. Brownsword, M. Hillenkamp, T. Laurent, R. K. Vaisa, H-R. Volpp, and J. Wolfrum, Chem. Phys. Lett. **266**, 1258 (1997).
[14] J. R. McNesby, J. Atmos. Sci. **26**, 594 (1969).
[15] N. S. Smith and F. Raulin, J. Geophys. Res. **104**, 1873 (1999).
[16] A. H. Laufer and J. R. McNesby, Can. J. Chem. **43**, 3487 (1965).
[17] B-M. Cheng, E. P. Chew, C-P. Liu, M. Bahou, Y-P. Lee, Y. L. Yung, and M. F. Gerstell, Geophys. Res. Lett. **26**, 3657 (1999).
[18] R. Bersohn and B. Katz, in *Isotope Effects in Gas-Phase Chemistry*, edited by J. A. Kaye, ACS Symposium Series, 502 (1992), p. 66.